Experimental Investigation of 3D Dynamical Effects in a Wake behind Circular Cylinder

Václav Uruba[1,2*], *Pavel* Procházka[1]

[1]Department of Fluid Dynamics, Institute of Thermomechanics, Czech Academy of Sciences, Dolejškova 5, 182 00, Prague, Czech Republic.
[2]Power System Engineering, Faculty of Mechanical Engineering, University of West Bohemia in Pilsen, Univerzitní 22, 306 14 Pilsen, Czech Republic.

Abstract. A circular cylinder in crossflow is subjected to the study of 3D dynamical structure of its wake. The typical dynamics is characterized by quasi-periodic behaviour called Kármán – Bénard vortex street with the typical frequency in dimensionless form known as Strouhal number. The experimental study relies on stereo Particle Image Velocimetry method, the plane of measurement is perpendicular to the flow in the distance 3.8 cylinder diameters in streamwise direction. Reynolds number was around 5 thousand. The structure and dynamical behaviour of the wake along the cylinder axis is studied in details. On the top of the known streamwise velocity deficit definition of the wake, the streamwise oriented dynamically evolving vortices are detected. For the detailed dynamics examination, the Oscillation Pattern Decomposition method was used. Waves of various structures travelling along the cylinder axis as well as some pulsations were identified. The wake dynamics is characterised by the streamwise velocity component deficit and the streamwise vorticity concentration. Both structures are moving periodically in transversal direction with the same frequency, the velocity deficit is shifted by a quarter of period behind the vorticity concentration in the shedding process.

1 Introduction

A circular cylinder in crossflow is a typical engineering problem, appearing in practice very often in various forms. In fluid mechanics, this case is considered as a typical canonical case, with relatively simple and straightforward boundary conditions, but complex structure of the flow. The wake is highly nonstationary and 3D in the same time.

In literature, extensive information resources could be found, starting from dawn of fluid mechanics until now. The first systematic work by von Kármán [1] followed by overview paper by Roshko [2], and Williamson [3] to mention the most cited. Interest of researches is not changing a lot during the time, however the technical means applied in the research, involving both experimental approach and mathematical modelling, develops substantially.

* Corresponding author: uruba@it.cas.cz

Recently we have appropriate means available for addressing even the most complex aspects of the phenomenon.

The wake dynamics has been simplified very often to a single-frequency, periodical process with 2D topology. The Kármán vortex street is defined and characterized by the single Strouhal frequency. The wake structure along the cylinder is considered to be synchronized, and thus 2D. In reality, this approach could be accepted for the fully laminar case only characterized by a very low Reynolds number (*Re*), bellow 150. For higher *Re* values the turbulence is present in the wake, the flow should be a broad-band process with random component and fully 3D topology. Neglecting 3D aspects could lead to fully unphysical conclusions, e.g. zero drag, so called d'Alembert's paradox, which could be resolved only by considering the 3D reality, see e.g. Hoffman, Johnson [4]. Some more ideas could be found e.g. in [5].

In the presented paper we are about to address the 3D aspects of the flow in the turbulent wake behind a long cylinder.

The general conclusions are valid not only for circular cylinders, but for cylinders with the different cross-sections as well, e.g. rectangular, the situation is qualitatively similar, see e.g. [6].

2 Description of experiments and analysis methods

The experiments were carried out in the Laboratory of Turbulent Shear Flows in the Institute of Thermomechanics ASCR, Prague. The existing flow-down facility with test section 250 x 250 mm^2. The generated flow was low turbulent level and regular. The facility is described in more details e.g. in [7].

2.1 Experimental setup

As a typical case we have chosen the circular cylinder with diameter $D = 15$ mm and the incoming velocity $U_e = 5$ m/s. The Reynolds number was thus around 5 thousand. The cylinder was sufficiently long (about 250 mm) to consider 2D boundary condition, its aspect ratio was about 16. The cylinder (in grey) and plane of measurement (in red) are shown in Figure 1.

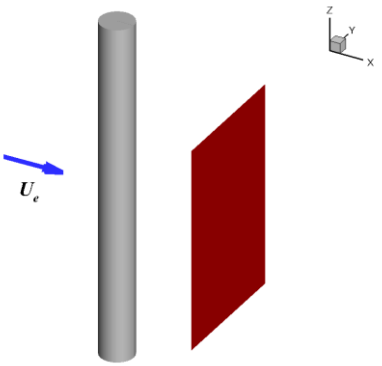

Fig. 1. Cylinder and plain of measurement.

The plane of measurement was chosen in the position 3.83 *D* downstream the cylinder axis. It was parallel to the cylinder axis and perpendicular to the incoming flow. The distance from the cylinder has been chosen just behind the "near wake", where the back-flow appears

temporarily. The situation could be compared with results of measurement in the streamwise plane of measurement, results were presented in [7].

2.2 Method of measurements

The Particle Image Velocimetry (PIV) method was applied in its stereo version. This method allows for evaluation of all 3 velocity components in the plane of measurement.

The measuring apparatus consists of laser and 2 CMOS cameras by Dantec Company. The laser is New Wave Pegasus, Nd:YLF double head with wavelength of 527 nm, with maximal frequency 10 kHz and shot energy of 10 mJ (for 1 kHz), thus the corresponding power is 10 W per one head. The 2 cameras VEO 410 with resolution of 1 280 x 800 pixels are able to acquire double-snaps with frequency up to 2 500 Hz (full resolution) and they use internal memory 16 GB each. The Scheinpflug mounting were used for the cameras lenses to get the focus planes identical with the laser-sheet plane. The situation is depicted in Figure 2.

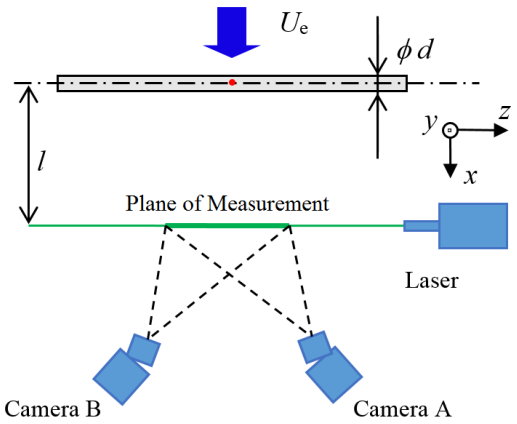

Fig. 2. Stereo PIV configuration.

Please note the Cartesian coordinate system in Figure 2 with origin on the cylinder axis (red dot), x in the streamwise direction and z is identical to the cylinder axis and y is perpendicular to both flow and cylinder axis.

The measurement records consist of 4 000 measurements performed with frequency 2 kHz. The Safex generator of particles in the form of oil droplets was used, the mean diameter of the particles was 1 μm, as shown in experimental studies by the apparatus supplier (see [11]). The data were acquired and post-processed using the Dynamic Studio and Tecplot softwares. The resolution of the field of interest was 94 x 56 vectors.

More details on the measuring technique are e.g. in [8].

2.3 Methods of data analysis

The methods of raw data evaluation and analysis are to be presented now.

The used statistical methods are based on averaging of acquired data over time. The mean values of the velocity components and Turbulent Kinetic Energy (*TKE*) distributions are to be presented. The *TKE* is defined as usual:

$$TKE = \frac{1}{2}\left(\overline{u^2} + \overline{v^2} + \overline{w^2}\right), \tag{1}$$

here u, v, and w are fluctuating parts of velocity components in x, y and z directions, respectively, the bar denotes averaging.

The Oscillation Pattern Decomposition (OPD) method has been used to study the flow-field dynamics, see [9]. The OPD method provides series of OPD modes, each OPD mode is characterized by the fluctuations topology in complex form (consisting of real and imaginary parts), frequency and attenuation of the pseudo-periodic (oscillating) behaviour. The fluctuations are expected in the form of cyclostationary process, when the real and imaginary topology appear in frequency of a mode quarter period, first positive and then negative velocity distributions. The Attenuation or amplitude decay is described by so called e-folding time representing the mean time period of the mode amplitude decay by factor "e". The other decay characteristic is the dimensionless "periodicity" which expresses the e-folding time in multiples of periods of the OPD mode defined by its frequency:

$$p = \tau_e \times f \ , \tag{2}$$

here p is periodicity, τ_e is e-folding time and f is the mode frequency.

The periodicity value could be considered as a measure of "relevance" of a given OPD mode. The frequency will be represented in dimensionless form as Strouhal number Sr:

$$Sr = \frac{f \times D}{U_i} \tag{3}$$

More details on the OPD method could be found in [9] and [10].

3 Results

The results of experiments are to be presented in 3 parts. First, analysis of the instantaneous topologies are to be shown, then the statistics, and finely the OPD analysis of the spatio-temporal data will be presented.

The plane of measurement (yz) will be shown, the cylinder axis is the line $y = 0$, in all graphs also the cylinder silhouette will be indicated by the broken lines $y = \pm 0.5$.

Please note that all coordinates are dimensionless, expressing numerically multiples of the cylinder diameter D. The velocities and TKE are normalised by U_e, while vorticity by the combination of D and U_e.

3.1 Acquired data

The quasi-periodical behaviour of the wake is characterized by the Strouhal frequency with corresponding Strouhal number $Sr = 0.21$. The Strouhal frequency was identified about 71 Hz. In the time-series of snapshots were selected situations corresponding to limiting positions of the wake.

Some of these situations are to be shown graphically in two forms. In both graphics the in-plane velocity vectors are to be shown. The first "velocity" form (a) shows the third, streamwise instantaneous velocity component u by colour map, this representation indicates the low-velocity fluid in the wake. In the second "vorticity" form (b), the colour represents the streamwise vorticity component, negative in blue and positive in red. This form shows presence the streamwise vortices in the instantaneous wake. To facilitate this identification, the vector-lines were added arbitrarily.

The 4 situations were selected to be presented, characterizing one period of the vortex shedding process. The wake is moving periodically from position y positive values to negative and back. We will show the situation in the following order: $y > 0$, $y = 0$, $y < 0$, $y = 0$. Those situations are shifted by a quarter of the shedding period.

The first example, snapshot No. 193, represents situation when the wake is located in top dead centre, close to the upper cylinder contour, y is positive. The situation is shown in Figure 3, the velocity form is on left (a) and the vorticity form on right (b). The vector lines constructed over the spanwise velocity components are used to make the streamwise vortical structures clearer. Please note strong streamwise vortices of both orientations distributed symmetrically around the cylinder axis, while the streamwise velocity deficit is shifted significantly upwards.

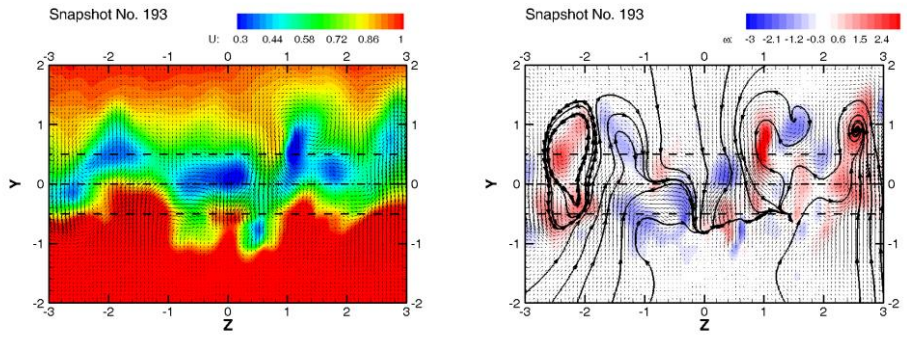

(a) (b)

Fig. 3. Instantaneous snapshot, wake shifted to the upper position. Streamwise velocity component distribution (a), streamwise vorticity component distribution (b).

Next stage is the central wake position, the wake is moving from up to down. In Figure 4a there is a snapshot No. 200 showing symmetrical wake in vertical direction, y is close to 0. However the vorticity distribution in Figure 4b suggests position of streamwise vortices on the level of lower cylinder contour y = -0.5, the upper part is nearly vortex-free.

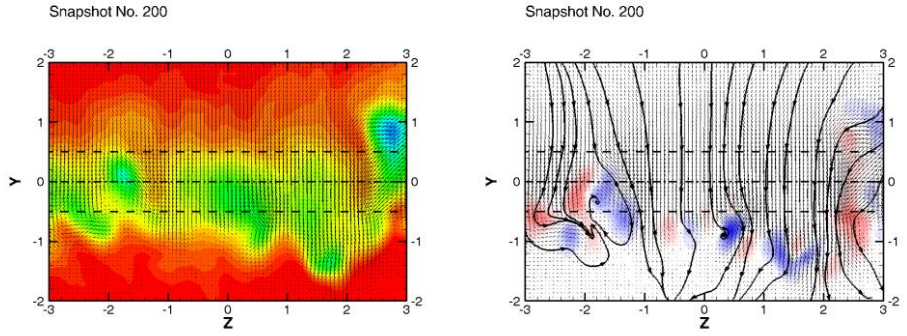

(a) (b)

Fig. 4. Instantaneous snapshot, wake in the middle position directed downwards. Streamwise velocity component distribution (a), streamwise vorticity component distribution (b).

The next position is represented by the snapshot No. 207 showing the situation when the wake is located close to the bottom dead centre, y is negative, see Figure 5a. The vorticity is distributed more-or-less symmetrically, similar to the situation when the wake is shifted to the upper position, compare to Figure 3b.

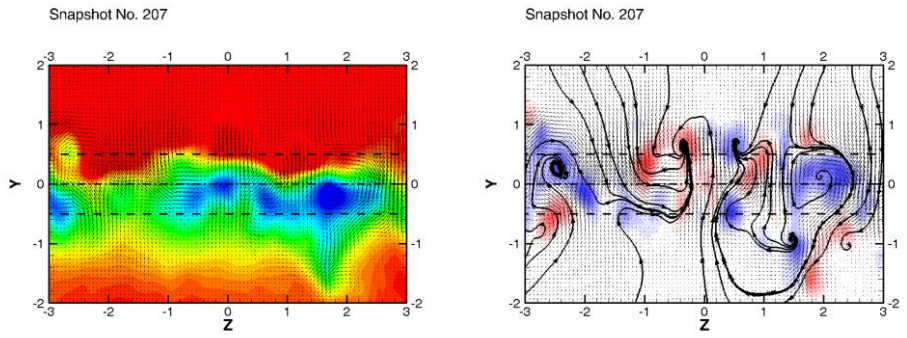

Fig. 5. Instantaneous snapshot, wake shifted to the lower position. Streamwise velocity component distribution (a), streamwise vorticity component distribution (b).

The last example in Figure 6 shows again the situation, when the wake is in the middle position, *y* is 0, but moving from down to up (snapshot No. 214), see Figure 6a. In this case the streamwise vortices are concentrated in the upper part above the cylinder, while the lower part is vortex-free, compare Figures 4b and 6b.

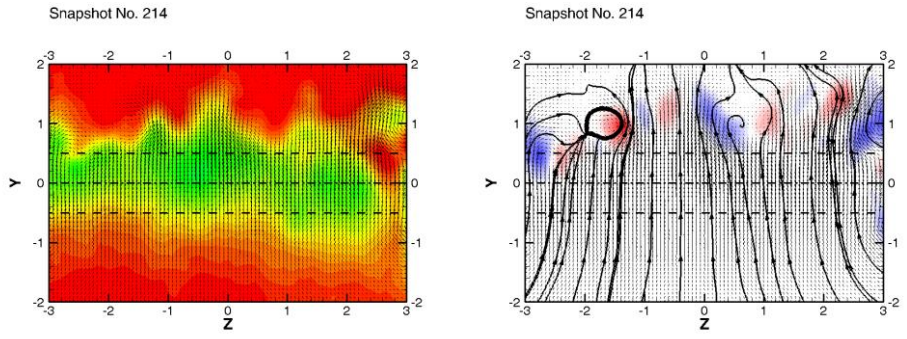

Fig. 6. Instantaneous snapshot, wake in the middle position directed upwards. Streamwise velocity component distribution (a), streamwise vorticity component distribution (b).

From the above presented results we could derive an important information on the wake structure and its dynamics.

The wake could be defined in two ways. First, the wake is defined as a streamwise velocity component deficit. We could recognize the random velocity fluctuations along the cylinder axis *z*. Those fluctuations are strong in the dead ends positions (Figures 3a, 5a), while in central positions, they are weak (see Figures 4a, 6a).

The second definition could rely on appearance of the streamwise oriented vortices with random distribution along the cylinder axis *z* and random vorticity sign, negative or positive. The vorticity concentration is much stronger in central positions (see Figures 3b, 5b) than close to dead ends (see Figures 4b, 6b).

Both structures, streamwise velocity component deficit and streamwise vorticity concentration, are moving periodically in transversal direction *y* with the same frequency.

However, the vorticity concentration is shifted by a quarter of period before the velocity deficit in the shedding process.

3.2 Statistics

Statistical analysis relies on averaging of instantaneous data series.

In Figure 7 the mean streamwise velocity component U (perpendicular to the plane of measurement) distribution is shown in the left-hand-part (a). Legend of U indicates values in multiples of U_e. The vector U_e is shown as a reference in left-upper corner, to demonstrate that the in-plane velocity components V and W are negligible.

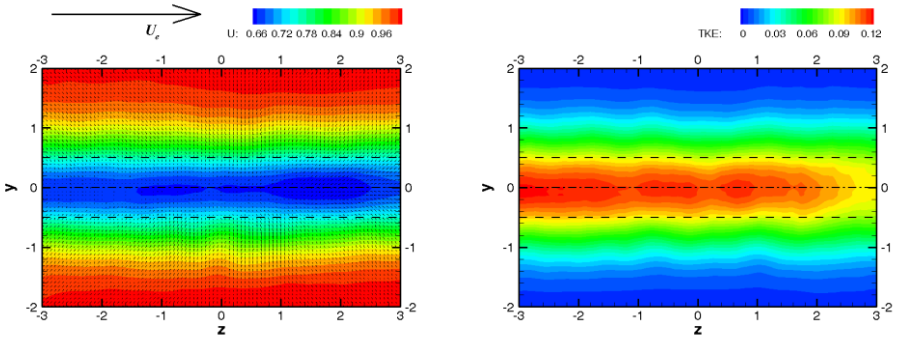

(a) (b)

Fig. 7. Mean streamwise velocity component (a), Turbulent Kinetic Energy (b) distributions.

The *TKE* distribution in Figure 7b shows the fluctuating activity maximum is located in the plane of symmetry $y = 0$ and it decays rapidly in transversal direction. In the position y = 2 the *TKE* approaches the free-stream value close to zero.

From Figure 7 it is clear, that the mean characteristics distributions, both U and *TKE*, are almost perfectly 2D, varying along the z axis of the cylinder insignificantly. The irregularities along the z-axis relate to experimental inaccuracy and limited statistical ensemble size (record of 2 s only).

3.3 Dynamics

The OPD analysis has been performed and 10 modes have been evaluated. Please note, that only fluctuations are analysed, the mean velocity field shown in Figure 7a is subtracted from the data set. This means, that the Reynolds decomposition into average and fluctuating parts of all quantities relevant to the problem is applied as a very first step.

In Figure 8 the OPD spectrum is shown in p-Sr plain. The dominant modes 1 and 2 are located around the shedding frequency $Sr_1 = 0.21$. The mode 3 is at a little higher frequency and the others higher order modes are of much lower frequencies.

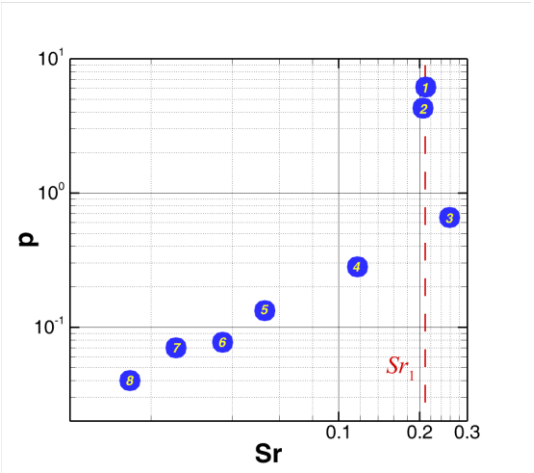

Fig. 8. OPD spectrum.

The first 5 OPD modes show not negligible values of periodicity, thus these modes are relevant as a part of cyclostationary process.

Next, the topologies of those relevant OPD modes are to be presented. The real part will be on the left (a) and the imaginary part on the right (b). The colour means here the out-of-plane velocity component *U*, positive in red and negative in blue. The in-plane velocity components are represented by arrows. Please note, that the absolute value of the fluctuating velocity components, both real and imaginary, has no direct physical meaning, as the modes are normalized. Only the topology is of relevance.

The first two OPD modes 1 and 2 are of the very same frequency and also the topology is very similar. It seems that these modes are in reality two versions of a single dominant mode. The real and imaginary parts are shown in Figures 9 and 10, respectively.

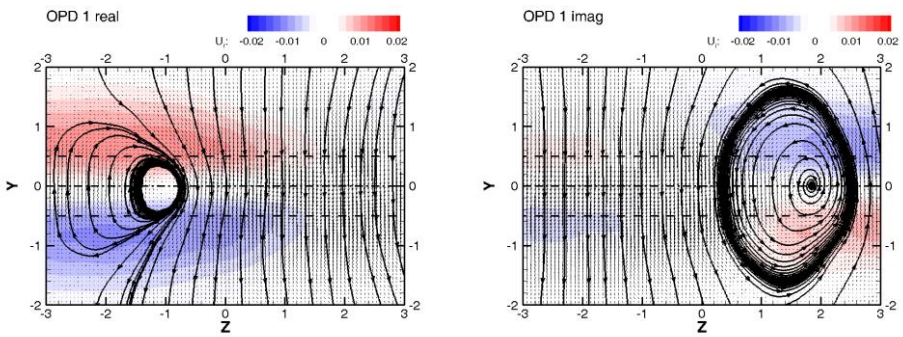

(a) (b)

Fig. 9. OPD mode 1, real (a) and imaginary (b) parts.

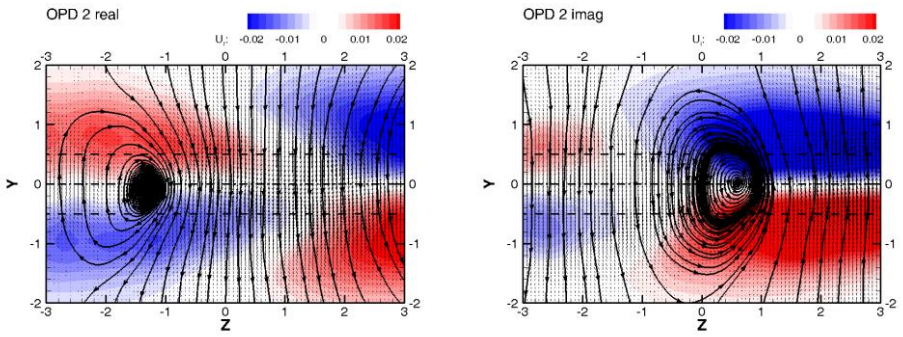

(a) (b)

Fig. 10. OPD mode 2, real (a) and imaginary (b) parts.

The dominant mode is formed by big velocity strips close to the cylinder silhouette, forming a chequered pattern, opposite orientation in upper – lower parts and right – left parts, respectively. On the top of that, the in-plane vortex is present, this means that the vortex has its axis in the streamwise direction *x*. Both the vortex and velocity strips are moving from the right to the left-hand-side forming the waves moving along the cylinder axis *z*. The frequency of this mode is close to the Strouhal frequency of the vortex street.

The OPD mod No. 3 is dominated by positive streamwise velocity component fluctuation close to the cylinder axis and negative fluctuations close to the cylinder silhouette. Those fluctuations form spots moving along the cylinder axis and changing the sign in the second half of the period. On the top of that, the weak flow in transversal *y* direction is present changing orientation during the period.

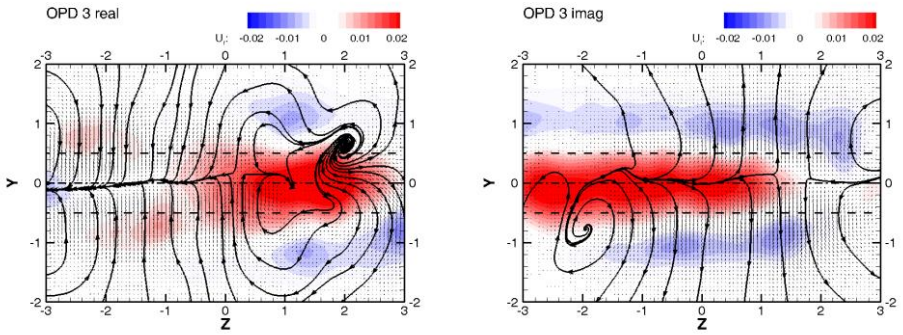

(a) (b)

Fig. 11. OPD mode 3, real (a) and imaginary (b) parts.

The topology of the next OPD mode No. 4 is shown in Figure 12. The 3 big vortices along the cylinder axis are moving along it in *z* direction. Those dominant structures are accompanied by system of pulsating jets on the cylinder's silhouette. The frequency is about one half of the Strouhal frequency.

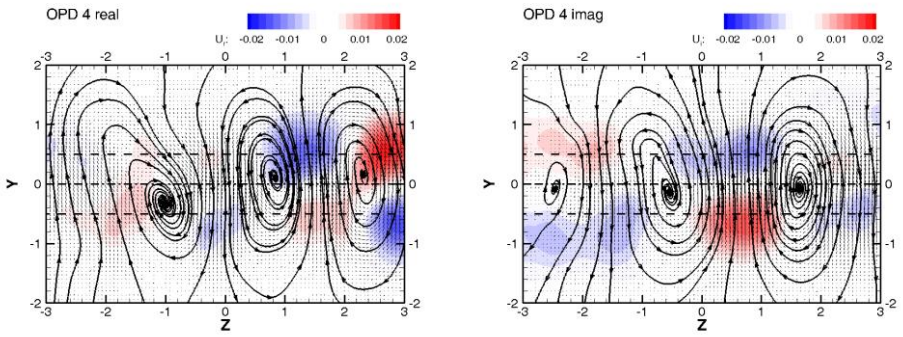

(a) (b)

Fig. 12. OPD mode 4, real (a) and imaginary (b) parts.

The last OPD mode presented here is the mode No. 5 in Figure 13. The mode is represented by the system of vortices and jets randomly distributed along the cylinder silhouette and changing theirs topology in time. There is no distinct motion along the axis *z*.

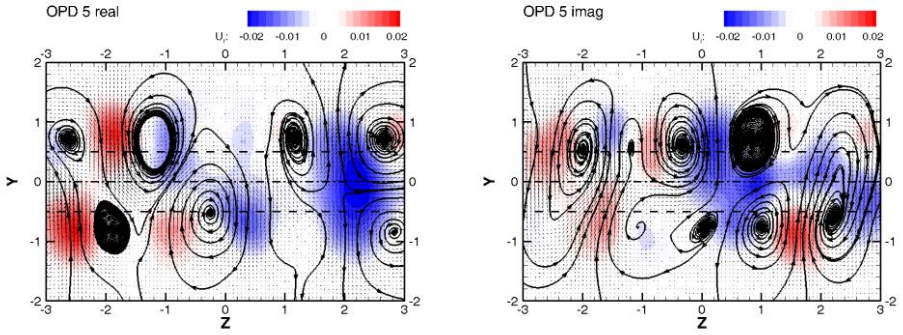

(a) (b)

Fig. 13. OPD mode 5, real (a) and imaginary (b) parts.

The higher OPD modes are significantly damped and thus not relevant to the overall dynamics.

4 Conclusions

The dynamical aspects of a fully turbulent wake behind a circular cylinder in cross-flow were studied experimentally using time resolved stereo PIV method. Reynolds number was about 5 thousand. Advanced methods of spatio-temporal data analysis have been used to gather a new information on the wake dynamics in 3D.

The results of the study show clearly, that despite the fact of presence 2D geometry, the flow in the wake is always 3D, at least its dynamical part. The time-mean structure could be 2D.

Typical dynamical patterns topology is presented in the paper. The wake is dominated by streamwise vortices appearing in distinct locations and phases of the quasi-periodical vortex shedding process randomly. Typical dynamics of those structures is wave motion along the

cylinder axis. The other distinct dynamical behaviour is connected with appearance streamwise velocity component fluctuating spots, which are again moving along the cylinder axis in waves, or they pulsate. Both dynamical structures in the wake, the streamwise velocity component deficit and the streamwise vorticity concentration, are moving periodically in transversal direction with the same frequency, the vorticity concentration is shifted by a quarter of period before the velocity deficit in the shedding process.

Acknowledgements

This publication was supported by the project of University of West Bohemia in Pilsen SGS-2022-023.

References

1. T. von Kármán, Aerodynamics. Columbus: McGraw-Hill. (1954)
2. A. Roshko, On the development of turbulent wakes from vortex streets. NACA Rep. 1191, pp.801-825. (1955)
3. C.H.K. Williamson, Vortex Dynamics in the Cylinder Wake, Annu. Rev. Fluid. Mech. **28**, pp. 477-539. (1996)
4. J. Hoffman, C. Johnson, Resolution of d'Alembert's paradox, J. Math. Fluid Mech., **12** 3, pp.321-334. (2010)
5. V. Uruba, On 3D instability of wake behind a cylinder, AIP Conference Proceedings, 1745, art. no. 020062. (2016)
6. V. Yanovych, D. Duda, V. Uruba, Structure turbulent flow behind a square cylinder with an angle of incidence, European Journal of Mechanics, B/Fluids, **85**, pp. 110-123, (2021)
7. V. Uruba, and P. Prochazka, On Harmonic Contents of the Wake behind a Circular Cylinder, 26th International Conference on Engineering Mechanics (IM), Engineering Mechanics 2020 (IM2020) , pp.500-503, (2020)
8. V. Uruba, P. Procházka, V. Skála, On the 3D Dynamics of the Wake Behind a Circular Cylinder, In Proceedings Topical Problems of Fluid Mechanics 2020, Prague, Edited by D. Šimurda and T. Bodnár, pp. 240-248, (2020)
9. V. Uruba, Decomposition methods in turbulent research, EPJ Web of Conferences, **25** 01095. (2012)
10. V. Uruba, Near Wake Dynamics around a Vibrating Airfoil by Means of PIV and Oscillation Pattern Decomposition at Reynolds Number of 65 000, Journal of Fluids and Structures, **55**, pp. 372-383. (2015)
11. DynamicStudio 7.4, User's Guide, Dantec Dynamics (2021)